Static and dynamic properties of a dimerized quantum-spin chain

1998 J. Phys.: Condens. Matter 10 6321

(http://iopscience.iop.org/0953-8984/10/28/013)

J. Phys.: Condens. Matter **10** (1998) 6321–6332. Printed in the UK PII: S0953-8984(98)93909-1

Static and dynamic properties of a dimerized quantum-spin chain

Oliver Fritz†, Stephen W Lovesey and Greg I Watson
ISIS Facility, Rutherford Appleton Laboratory, Oxfordshire OX11 0QX, UK

Received 29 April 1998

Abstract. Various static spin-correlation functions and the weights of the spin excitations, or collective normal modes, in the van Hove response function, observed in neutron scattering experiments, are calculated as a function of temperature for a model quantum-spin chain. The spins interact through an isotropic Heisenberg exchange that extends to nearest-neighbour spins. In our model, spins of magnitude 1/2 form a dimerized chain with alternating exchange interactions. We explore the static and dynamic properties for ferromagnetic and antiferromagnetic exchange interactions. Results for the various properties are shown to be exact in the limit of a high temperature, and we argue that the results are very good at low temperatures. Unlike the case for linear spin-wave theory, the results are also exact in the limit of strong dimerization, i.e. non-interacting coupled pairs of spins.

1. Introduction

Recent experimental progress in the investigation of low-lying excitations in one-dimensional spin-1/2 Heisenberg chains has led to renewed interest in theoretical approaches to model systems. Special attention is given to systems where, either through a spin-Peierls transition, as in the compounds $CuGeO_3$ [1] and NaV_2O_5 [2], or through an intrinsic structural asymmetry, as in $CuWO_4$ [3] and $(VO)_2P_2O_7$ [4], the effective intra-chain antiferromagnetic interactions alternate in strength. The materials can show no magnetic order at all ($CuGeO_3$), or, due to inter-chain coupling, long-range antiferromagnetic order ($CuWO_4$). In the absence of magnetic order, the ground state of an isolated chain is well described by a 'dimer state', which consists of adjacent pairs of spins coupled into singlets. The dimer state has total spin zero, and a gap to low-lying excitations, because of the energy required to excite a singlet dimer to a triplet. Assuming that such local excitations acquire dispersion by hopping from one dimer to the next, a quantitative account of the well-defined magnon peak observed in neutron scattering can be given [5, 6]. This picture provides an appealing intuitive interpretation of the energy gap at the centre of the Brillouin zone and of the threefold degeneracy of the excitations, and is exact in the limit of strong dimerization. Conventional spin-wave theory, applied to the paramagnetic state where expectation values of products of spin operators display a full rotational symmetry, cannot readily account for these features.

Neither the spin-wave nor the dimer theory addresses the observed continuum component of the spectrum. This has been interpreted as a two-magnon continuum, or alternatively as a two-soliton continuum [7]. In the dimerized chain, a soliton may be

† Present address: Paul Scherrer Institut, CH-5232 Villigen PSI, Switzerland.

0953-8984/98/286321+12$19.50

envisioned as a single unpaired spin, separating segments of singlet pairs. However, these solitons are subject to a confining effective potential [8], and are always bound in pairs; in this picture, a magnon is a triplet two-soliton bound state. Thus, a two-soliton continuum is possible only in the case of a spin-Peierls chain, and requires a generalization of the model considered here, to include the phonon coupling responsible for spontaneous dimerization. An exception is the limit of a regular (undimerized) chain, such as $KCuF_3$ [9], in which the confining potential vanishes, the solitons unbind and the magnon peak is replaced by a two-soliton continuum. A full understanding of the excitation spectrum of dimerized chains might be revealed with a combination of techniques, including field theories and numerical simulations. A review completed in 1981 of various theories on this subject is found in reference [10].

Apart from the dimerized antiferromagnetic chain, one may also consider its ferromagnetic counterpart, and also a 'mixed' chain where the couplings alternate in sign as well as magnitude. Whereas the ferromagnetic case is less well studied, $Sr_{14}Cu_{24}O_{41}$ has recently been proposed as a candidate for having a mixed-chain structure [11], and first successful neutron scattering experiments have been performed with single crystals of this material [12, 13]. Furthermore, there are a number of organic compounds [14, 15] which can be described by a mixed-chain model. Past theoretical work on the mixed chain [16] has, apart from an investigation of the limit of weakly ferromagnetically coupled antiferromagnetic dimers [17], concentrated on the connection with the $S = 1$ 'Haldane gap' system.

The theory presented in this paper treats a dimerized chain of Heisenberg spins $S = 1/2$ with full rotational symmetry and no long-range magnetic order. It can be applied for an arbitrary strength of the dimerization, is, unlike spin-wave theory, correct in the limit of isolated dimers, and the expected results are recovered in the limit of a regular chain. It does not address the continuum part of the spectrum. We show that our results are good in an interval of temperatures of interest in the interpretation of available experimental data. In the limit of an infinite temperature, no approximation in the results remains.

In the following section we define the model and describe the method of closing the infinite hierarchy of equations of motion for the spin operators. Thereafter, in sections 3 and 4, one finds our expressions for the static spin-correlation functions, the wave-vector-dependent isothermal susceptibility, and the spectral weights of the spin excitations in the van Hove response function observed in neutron scattering experiments. Results for these quantities are found in sections 5 and 6: first a collection of analytic results valid at the two extremes of the temperature, and, secondly, extensive results at intermediate temperatures obtained by numerical analysis. Our conclusions are gathered in section 7.

2. The model and equations of motion

Quantum-spin operators placed at lattice sites in a chain interact by a Heisenberg exchange mechanism of alternating strength J and αJ. It is convenient to employ two spin operators, $\boldsymbol{S}$ and $\boldsymbol{T}$, of equal magnitude 1/2, placed at alternate sites in the chain. The Hamiltonian of the dimerized chain is

$$H = J \sum_l \{\boldsymbol{S}_l \cdot \boldsymbol{T}_{l+1} + \alpha \boldsymbol{S}_{l+1} \cdot \boldsymbol{T}_{l+1}\} \tag{1}$$

where $l = 0, \pm 1, \ldots$. We will consider also a regular Heisenberg chain whose Hamiltonian is obtained from (1) by setting $\alpha = 1$.

To study the dynamic and static properties of the model, we construct the equation of motion for the spin-ladder operators $S^+ = S^x + \mathrm{i}S^y$, and T^+. This is the first equation of an infinite hierarchy of equations for the time development. We close the set of equations at the second level, following a scheme used by Kondo and Yamaji [18] in their study of a regular chain, with $\alpha = 1$.

In constructing the equations, one uses $\langle S^\alpha \rangle = 0$, since there is no long-range magnetic order. The model is isotropic in the spin space, so $\langle S^x S^y \rangle = \langle S^y S^z \rangle = \langle S^z S^x \rangle = 0$, and $\langle S_a^\alpha S_b^\alpha \rangle$ is independent of the Cartesian label. Furthermore, $\langle S_a^+ S_b^- \rangle = \langle S_a^- S_b^+ \rangle = 2\langle S_a^z S_b^z \rangle$.

Following a standard prescription [18, 19] an expression for the van Hove response function $S(q, \omega)$ is obtained from the approximate equations of motion. This expression contains a number of correlation functions as parameters. Through a Fourier transform over the Brillouin zone these correlation functions are recovered from $S(q, \omega)$, and their values are thus determined by a self-consistency condition. At a temperature large compared to $|J|$, solutions for the correlation functions are found by analytic methods. A numerical method is used to determine the self-consistent solutions at an arbitrary temperature, T, which can be checked against the analytic results for $T \gg |J|$. A few analytic results have also been obtained for $T \ll |J|$ and for correlation functions of large spatial index.

3. Self-consistent equations

The spin operators $\boldsymbol{S}$ and $\boldsymbol{T}$ in (1) have a magnitude 1/2. In the equations of motion for S^+ and T^+ we use $(S^+)^2 = (S^-)^2 = 0$ and $(S^z)^2 = 1/4$, and the corresponding identities for $\boldsymbol{T}$. The equations of motion, obtained by closure at the second level, contain three correlation functions:

$$A_1 = \langle S_l^z T_{l+1}^z \rangle \qquad A_1' = A_{-1} = \langle S_l^z T_l^z \rangle \tag{2a}$$

and

$$A_2 = \langle S_l^z S_{l+1}^z \rangle = \langle T_l^z T_{l+1}^z \rangle. \tag{2b}$$

For $\alpha = 1$ one has $A_1 = A_1'$. A fourth thermodynamic variable, denoted by ξ, arises in the mechanism chosen to close the hierarchy of equations, e.g.,

$$S_l^z S_{l+1}^z T_{l+1}^+ \approx \xi \langle S_l^z S_{l+1}^z \rangle T_{l+1}^+ = \xi A_2 T_{l+1}^+. \tag{3}$$

The introduction of the variable ξ is essential for the success of our approach. Without this variable, the self-consistency equations would overdefine the correlation functions [20, 21].

It is interesting to enquire whether the closure of the equations of motion that we adopt can be successfully applied to spins $S > 1/2$. We have concluded that closure at the second level, used here, applied to $S > 1/2$ is not robust and entails a larger degree of approximation than found in our case of $S = 1/2$. This view is reached by consideration of terms in the second equation of motion that are zero for $S = 1/2$, e.g. $(S^+)^2 S_a$. To reach the same situation for $S = 1$, say, one needs $(S^+)^3 S_a$ and this may first occur at the third level in the hierarchy of equations of motion. So, to achieve the level of approximation that we have for $S = 1/2$ with spins of a larger magnitude, one must close the hierarchy at the third or higher level.

Our model possesses the obvious property that it is unchanged with the transformation

$$\begin{aligned} &\alpha \to 1/\alpha \qquad J \to \alpha J \\ &A_1 \to A_1' \qquad A_1' \to A_1 \qquad A_2 \to A_2. \end{aligned} \tag{4}$$

This transformation is nothing but an inversion of the lattice around a site and a rescaling of the exchange interactions. We can express this invariance in a more general form as

follows: $A_n = A'_{-n}$ for odd integer n, and $A_n = A_{-n}$ for even n. Note that the index n, unlike l in the Hamiltonian (1), counts the total number of bonds between any two spins in the chain. Under the transformation, we find $\xi \to \xi$; cf. (14).

The normal-mode frequencies, and the transcendental equations for A_1, A'_1, A_2, and ξ are couched in terms of the following quantities. Let $\tilde{A}_n = \xi A_n$, and

$$\begin{aligned} f &= \frac{1}{2} + 2\alpha\tilde{A}'_1 + 2\alpha\tilde{A}_2 \qquad & g &= \frac{1}{2}\alpha + 2\tilde{A}_1 + 2\tilde{A}_2 \\ \Delta &= 2\alpha(\tilde{A}_1 - \tilde{A}'_1) & h &= \frac{1}{2}(1+\alpha^2) + 4\alpha\tilde{A}_2. \end{aligned} \tag{5}$$

Defining

$$C = J^2\sqrt{(\alpha g + f)^2 + 2\alpha g f(\cos q - 1) - (\Delta \sin q)^2} \tag{6}$$

where q is a wave-vector in units of the inverse of the distance between two neighbouring $\boldsymbol{S}$, or $\boldsymbol{T}$, the four normal-mode frequencies satisfy

$$\omega^2_{a,b} = J^2(h + 2\alpha(\tilde{A}_1 + \tilde{A}'_1)\cos q) \pm C. \tag{7}$$

Quantities with an index a have to be evaluated using $+C$, and those with an index b have to be evaluated using $-C$. For $q = 0$ we find $\omega_a \neq 0$, and $\omega_b = 0$. With $\alpha = 1$ the modes cross at $q = \pi$, and the physically relevant mode is ω_b for $0 < q < \pi$ and is ω_a for $\pi < q < 2\pi$, recovering the result for the regular chain [18] in a doubled Brillouin zone; cf. figures 1 and 5, later. In the limit $\alpha = 0$ one finds $\omega_a = 1$ and $\omega_b = 0$, which follow from the results $A'_1 = A_2 = 0$ and $A_1 = -1/4$. For a small value of α, we find

$$\omega_a \approx J(1 + 2\alpha\tilde{A}_1 \cos q). \tag{8}$$

Next we consider the transcendental equations that follow by calculating any two-spin correlation function from the approximate equations of motion. For a temperature T, expressed by $\beta = 1/k_B T$, we find that

$$A_n = \frac{1}{4\pi}\int_0^{2\pi} \frac{\mathrm{d}q}{C}\left\{\frac{\coth(\beta\omega_a/2)}{\omega_a}G_a(q) - \frac{\coth(\beta\omega_b/2)}{\omega_b}G_b(q)\right\}. \tag{9}$$

For $n = 0, 2, 4, \ldots$, the $G_{a,b}(q)$ read

$$G_{a,b}(q) = -J^3 \cos\frac{nq}{2}\{(\pm C/J^2)(A_1 + \alpha A'_1) + \alpha g(A_1 \cos q + \alpha A'_1) + f(A_1 + \alpha A'_1 \cos q)\} \tag{10}$$

and for $n = \pm 1, \pm 3, \ldots$, they read

$$\begin{aligned} G_{a,b}(q) = {} & J^3 \cos\frac{(n-1)q}{2}\{(\pm C/J^2)A_1 + f(A_1 + \alpha A'_1) + \Delta(A_1 \cos q + \alpha A'_1)\} \\ & + J^3 \cos\frac{(n+1)q}{2}\{(\pm C/J^2)\alpha A'_1 + \alpha g(A_1 + \alpha A'_1) - \Delta(A_1 + \alpha A'_1 \cos q)\} \end{aligned} \tag{11}$$

where, again, indices a and b refer to the sign of C. Setting $n = 0$ and $n = 2$ in (10), and $n = \pm 1$ in (11), and thereby recovering A_0, A_2, A_1, and A'_1, respectively, we obtain the four equations that are solved self-consistently. For completeness, we give $G_{a,b}$ for A_1 and A'_1 from (11) in a simpler form as

$$G^{A_1}_{a,b}(q) = J^3\{(\pm C/J^2)(A_1 + \alpha A'_1 \cos q) + \alpha A'_1 \Delta \sin^2 q + (A_1 + \alpha A'_1)(\alpha g \cos q + f)\} \tag{12}$$

for A_1, and

$$G_{a,b}^{A_1'}(q) = J^3\{(\pm C/J^2)(\alpha A_1' + A_1\cos q) - A_1\Delta\sin^2 q + (A_1 + \alpha A_1')(\alpha g + f\cos q)\} \tag{13}$$

for A_1'. One more relation arising from the symmetry of our model is

$$A_1' - \alpha A_1 + 4\xi\{A_1A_1'(\alpha - 1) + A_2(\alpha A_1' - A_1)\} = 0. \tag{14}$$

We derive this by requiring A_n for n even to be an invariant under the transformation in (4), and we deduce that $\xi \to \xi$.

4. Observable quantities

The quantity observed by inelastic neutron scattering is the van Hove response, a function of wave-vector and frequency:

$$S(q,\omega) = \frac{1}{2\pi}\int_{-\infty}^{\infty} \mathrm{d}t\ \exp(-\mathrm{i}\omega t)\sum_{m,m'} \mathrm{e}^{\mathrm{i}q(m'-m)}\langle S_m^+(0)S_{m'}^-(t)\rangle \tag{15}$$

where m and m' range over every site in the chain. At this point it is important to note that we assume a regular spacing throughout the whole lattice in spite of an alternating exchange interaction. This is in agreement with the very small observed lattice distortion, e.g., in $CuGeO_3$, but not necessarily true for structurally dimerized materials, an example of which is $(VO)_2P_2O_7$. However, only q-dependent quantities derived from (15) are affected by a lattice distortion, and, for the purpose of clarity, we have omitted the resulting more complicated expressions for observable quantities like (16) and (19). Real-space correlation functions remain unaffected by a lattice distortion.

Since the normal modes are undamped, at the level of approximation that we employ, they make contributions to the van Hove response that have a dependence on frequency given by $\delta(\omega \pm \omega_a)$ and $\delta(\omega \pm \omega_b)$. The two δ-functions for the creation events, $\delta(\omega - \omega_{a,b})$ are, apart from the detailed-balance factor $1 + n(\omega)$, accompanied by the spectral-weight functions, given per spin:

$$\mathcal{F}_{a,b}(q) = -J^3\frac{F_{a,b}}{\pm C\omega_{a,b}}\left(1 - \cos\frac{q}{2}\right) \tag{16}$$

where

$$\begin{aligned} F_{a,b}(q) = {} & (A_1 + \alpha A_1')\left(\pm C/J^2 + \alpha g - f - 2f\cos\frac{q}{2}\right) \\ & + 2\Delta(A_1 - \alpha A_1')\cos\frac{q}{2}\left(1 + \cos\frac{q}{2}\right) - 2A_1(\alpha g - f)\left(1 + \cos\frac{q}{2}\right). \end{aligned} \tag{17}$$

Again, quantities with an index a involve $+C$, and quantities with an index b involve $-C$. For small values of α, we get

$$\mathcal{F}_a \approx -2A_1\left(1 - \cos\frac{q}{2}\right)(1 - 2\alpha\tilde{A}_1\cos q). \tag{18}$$

Finally, we can derive the wave-vector-dependent susceptibility $\chi(q)$ per spin from the relation

$$\chi(q) = \int_{-\infty}^{\infty}\frac{\mathrm{d}\omega}{\omega}\ S(q,\omega) = \int_0^{\infty}\frac{\mathrm{d}\omega}{\omega}\ \frac{S(q,\omega)}{1 + n(\omega)} = \frac{\mathcal{F}_a}{\omega_a} + \frac{\mathcal{F}_b}{\omega_b}. \tag{19}$$

The absence of the usual factor 2 in the right-hand side of the first equality in (19) stems from the fact that we give the susceptibility for correlations $\langle S^z S^z \rangle_q$, which are half the value of $\langle S^+ S^- \rangle_q$, used in (15) and (16).

Results obtained from our model by setting $\alpha = 0$ are easy to derive. It can be shown that the foregoing expressions evaluated for $\alpha = 0$ reproduce those results. Also, setting $\alpha = 1$ we recover all of the expressions provided for the regular chain as given in [18]. The authors of [18] did not consider the spectral weights (16), the susceptibility (19), or the dimerized chain.

5. Analytic results

First we give the static susceptibility in terms of the correlation functions A_n for arbitrary temperature. We find for $q = 0$

$$\chi(0) = \frac{-4A_1}{J} \frac{(\alpha + 4\tilde{A}_1' + 4\tilde{A}_2)}{(\alpha - 4\tilde{A}_1' + 4\tilde{A}_2)(1 - 4\alpha\tilde{A}_1 + 4\alpha\tilde{A}_2) - 64\alpha\tilde{A}_1\tilde{A}_1'} \tag{20}$$

and for $q = \pi$

$$\chi(\pi) = \frac{-4A_1}{J} \frac{(\alpha - 4\tilde{A}_1' + 4\tilde{A}_2)}{(\alpha - 4\tilde{A}_1' + 4\tilde{A}_2)(1 - 4\alpha\tilde{A}_1 + 4\alpha\tilde{A}_2)}. \tag{21}$$

In the limit $T \gg |J|$, the leading-order terms in an expansion of A_1, A_1', and A_2 in terms of βJ are found to be

$$A_1 = \frac{-1}{16}\beta J \qquad A_1' = \frac{-\alpha}{16}\beta J \qquad A_2 = \frac{\alpha}{64}(\beta J)^2. \tag{22}$$

These results are identical to results obtained by an independent calculation of the correlation functions that uses an expansion of $\exp(-\beta H)$, e.g.,

$$A_1 = -\beta J\left(\frac{1}{3}S(S+1)\right)^2. \tag{23}$$

For ξ we find from (14) and (22) the value $\xi = 1$ in this limit. Equally, the susceptibility χ can be derived. It becomes independent of the wave-vector, and approaches the well-known result

$$\chi = \frac{1}{4}\beta = \frac{S(S+1)}{3}\beta. \tag{24}$$

On the low-temperature side, analytic results can be derived for $\alpha = 1$, and they coincide with those given in reference [18]. For arbitrary α, the leading-order behaviour for large n can be derived from (9), (10), and (11). In all cases these show at non-zero temperature an exponential decay, with a correlation length which diverges as $T \to 0$. For the pure ferromagnet ($J < 0, \alpha > 0$) at $T = 0$, we find $A_n = 1/12$ for all $n \neq 0$, as expected for a saturated ferromagnetic ground state. In all other cases, at $T = 0$, we find $A_n \propto 1/n^2$ for large n, i.e. an algebraic decay of correlations. This may be compared with the exact result (p 160 in [22]) for the regular Heisenberg antiferromagnet ($J > 0, \alpha = 1$), namely $A_n \propto (\ln n)^{1/2}/n$. In this case our theory correctly shows algebraic decay of correlations in the ground state, but underestimates the strength of short-range correlations.

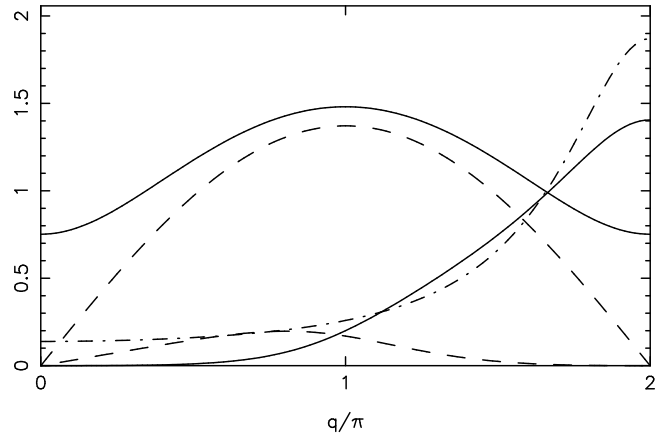

Figure 1. Normal modes $\omega_{a,b}$ (symmetric around $q = \pi$) and the respective spectral weights $\mathcal{F}_{a,b}$ for $J = 1$ and $\alpha = 0.9$ at $T \ll |J|$. Solid lines are ω_a and $\mathcal{F}_a$, dashed lines are ω_b and $\mathcal{F}_b$. Also given is the wave-vector-dependent susceptibility $\chi(q)$ (dash-dotted line) as defined in (19).

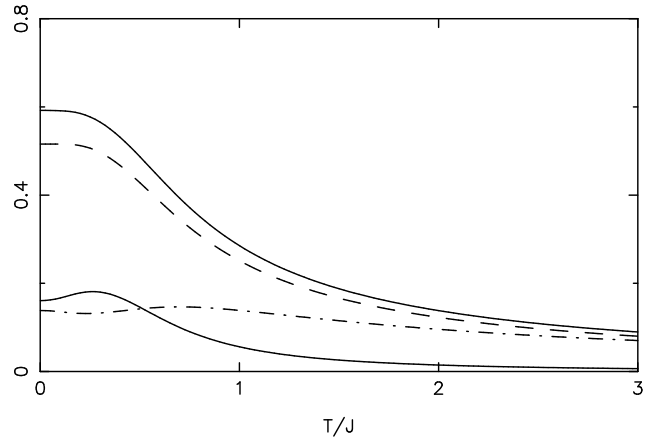

Figure 2. Correlation functions $4|A_1|$ (upper solid line), $4A_2$ (lower solid line), and $4|A_1'|$ (dashed line), and $q = 0$ susceptibility (dash-dotted line) for $J = 1$ and $\alpha = 0.9$.

6. Numerical results

For an arbitrary temperature, equations (9), (10), (12), (13), and (14) are solved numerically. We discuss the numerical results in three representative cases. In each case, we give an example of the normal-mode dispersion relations, the spectral weights, and the wave-vector-dependent susceptibility (figures 1, 3, 5). Owing to our choice of the length scale and the fact that we have two spins per unit cell, the normal modes $\omega_{a,b}$ have a period of 2π and are symmetric around $q = \pi$, whereas the spectral weights $\mathcal{F}_{a,b}$ and the susceptibility $\chi(q)$ have a period of 4π and are symmetric around $q = 2\pi$. The temperature dependence of the correlation functions and static susceptibilities for a range $0 < T < 3J$ appear in figures 2, 4, 6. Note, that the correlation functions are multiplied by a factor of 4 in the plots, in accordance with the practice of normalizing the same-site correlation function

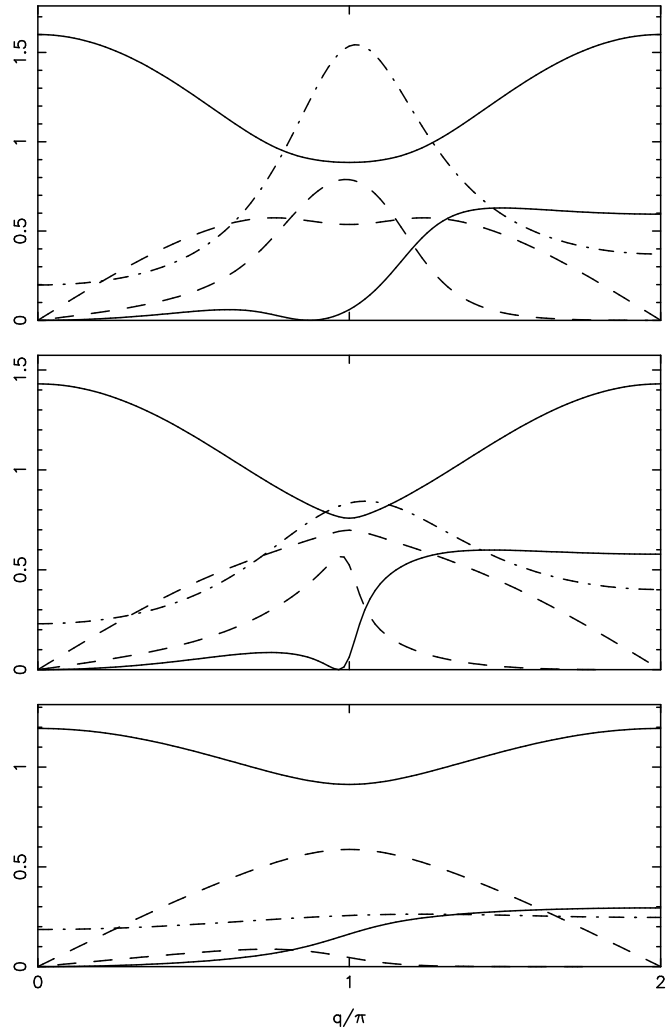

Figure 3. Temperature dependence of the spectrum. Top to bottom: $T = 0$, $T = 0.3J$, $T = J$. Given are normal modes $\omega_{a,b}$ (symmetric around $q = \pi$) and the respective spectral weights $\mathcal{F}_{a,b}$ for $J = 1$ and $\alpha = -0.5$. Solid lines are ω_a and $\mathcal{F}_a$, dashed lines are ω_b and $\mathcal{F}_b$. Also given is the wave-vector-dependent susceptibility $\chi(q)$ (dash-dotted line).

$A_0 = S(S+1)/3 = 1/4$ to the value of 1, and the fact that $k_B = 1$ in all plots. We only consider cases with $|\alpha| < 1$, as the parameter space $|\alpha| > 1$ can be mapped to $|\alpha| < 1$ by use of the transformation (4).

Common to all temperature-dependent plots (figures 2, 4, 6) is the observation that already for $T \geqslant J$, the correlation functions and the susceptibility agree well with their analytic high-temperature expansions. At low temperatures, one can distinguish clearly between antiferromagnetic correlations showing a maximum at $T \approx 0.3J$ (figure 2 and A_1' in figure 4), and ferromagnetic correlations reaching their highest values at $T = 0$ (figure 6 and A_1 in figure 4). This feature has already been observed in reference [18], and seems to be characteristic to our results. The plots of the normal modes and spectral weights reveal the nature of the local order as expected from the respective signs of J and α. These

quantities are plotted at temperatures $T \ll |J|$, in order to reveal their structure more clearly. We observe that varying the temperature on an energy scale of αJ has a minor influence on the plotted quantities, i.e. the relevant energy scale for the temperature dependence of the observed quantities seems to be the larger of J and αJ, which in our case is always J.

Figures 1 and 2 refer to the 'pure' antiferromagnetic chain, i.e., a chain with $J > 0$ and $\alpha > 0$. From figure 1, the behaviour in the limit $\alpha \to 1$ can be seen as the normal modes become degenerate at $q = \pi$ and the spectral weights select the relevant mode for $q < \pi$ and $q > \pi$, respectively. The susceptibility peaks at $q = 2\pi$, i.e., the antiferromagnetic point. The contribution to the scattering at that point comes from the gapped branch ω_a. The approximations made in our theory do not allow the lower branch ω_b to have a gap at $q = 0$, i.e. the lower branch is reminiscent of a Goldstone mode. In consequence, the susceptibility does not decay exponentially at very low temperatures, but remains finite (figure 2). The sum of the spectral weights $\mathcal{F}_a + \mathcal{F}_b$, i.e. the integrated neutron scattering intensity, has a finite slope at $q = 0$ and agrees qualitatively with experiments performed at low temperatures (figure 10 in [1]). Looking at figure 1, at higher temperatures the displayed quantities are smaller and show less dispersion, and no radical new effects emerge.

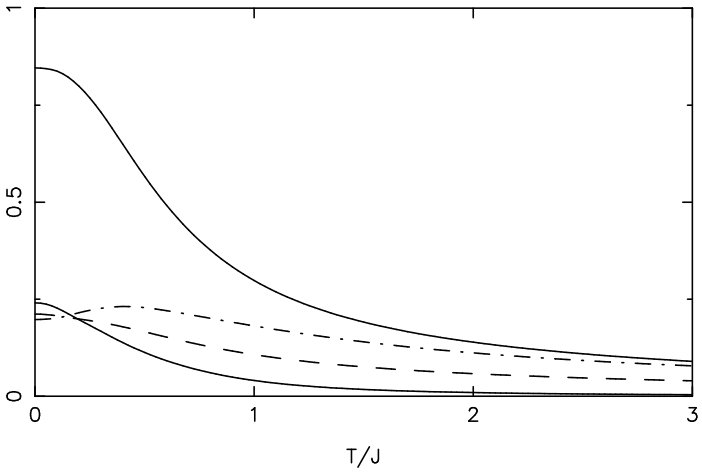

Figure 4. The correlation functions $4|A_1|$ (upper solid line), $4|A_2|$ (lower solid line), and $4A_1'$ (dashed line), and $q = 0$ susceptibility (dash-dotted line) for $J = 1$ and $\alpha = -0.5$.

The next case (figures 3, 4) is a 'mixed' chain of antiferromagnetic bonds alternating with ferromagnetic bonds ($J > 0, \alpha < 0$). The maxima in the susceptibility $\chi(q)$ at $q = \pi$ and $q = 3\pi$ indicate a locally ordered two-up–two-down spin pattern. Note that the spectral weight for ω_b vanishes at $q = 0$ and $q = 2\pi$, and mimics the q-dependence of $\chi(q)$. In figure 3, we have also given representative plots of the spectra for three different temperatures (increasing from top to bottom). With increasing temperature the susceptibility becomes independent of q and approaches its high-temperature value of $\beta/4$ over the whole range of the Brillouin zone.

Finally, a pure ferromagnetic chain ($J < 0, \alpha > 0$) is given in figures 5 and 6. As expected for a ferromagnetically ordered chain at $T = 0$, the correlation functions A_1, A_1', and A_2 take the value of 1/12, irrespective of the coupling constants J and α. This result can also be derived analytically from our equations. Consequently, the susceptibility diverges at $q = 0$ for small T as $1/T$.

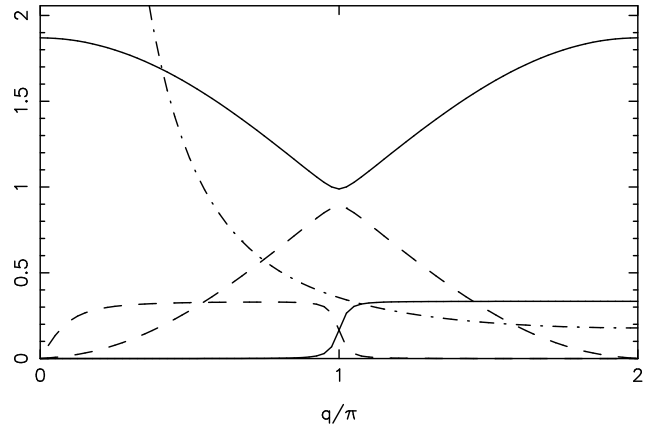

Figure 5. Normal modes $\omega_{a,b}$ (symmetric around $q = \pi$) and the respective spectral weights $\mathcal{F}_{a,b}$ for $J = -1$ and $\alpha = 0.9$ at $T \ll |J|$. Solid lines are ω_a and $\mathcal{F}_a$, dashed lines are ω_b and $\mathcal{F}_b$. Also given is the wave-vector-dependent susceptibility $\chi(q)$ (dash-dotted line).

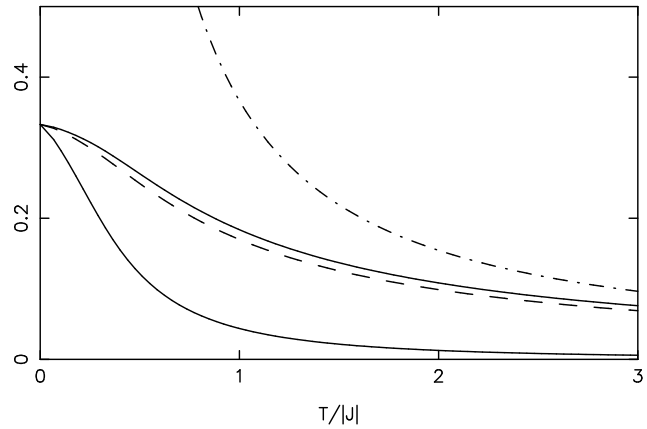

Figure 6. The correlation functions $4A_1$ (upper solid line), $4A_2$ (lower solid line), and $4A_1'$ (dashed line), and $q = 0$ susceptibility (dash-dotted line) for $J = -1$ and $\alpha = 0.9$.

7. Conclusions

Our theoretical approach to the dimerized chain provides useful results for quantities observed in neutron scattering experiments. In addition, we provide a number of analytic expressions for various quantities shown to be correct for certain points in the parameter space of J, α, and T. It must be emphasized that *a priori* the quality of our theory does not depend on the size and sign of α, and we demonstrate that it is exact for $\alpha = 0$. We provide expressions for observable quantities like the van Hove response and the susceptibility in terms of the correlation functions A_1, A_1', and A_2, and the model parameters J and α at arbitrary temperatures, and our theory therefore enables the experiments to be interpreted in a straightforward manner.

For the case of the antiferromagnetic chain, in our theory a gapless branch is always present for any non-zero α. The gapless mode is the analogue of a Goldstone mode for a system without long-range order, and is unavoidable with our chosen scheme for linearizing

the dynamical equations. However, it is known that the dimerized spin chain has a gapped spectrum unless $\alpha = 1$. The resolution of this problem lies in the weights assigned to these modes. Indeed, the gapless branch has no weight in it at the points of high symmetry in the Brillouin zone, and in all cases the predicted properties are dominated by the gapped branch of the spectrum. The gapped branch is absent altogether for $\alpha = 0$, and in this limit, as well as for high temperatures, the theory becomes exact. For the regular ($\alpha = 1$) antiferromagnet, the decay of correlations with increasing distance compares well with exact results. The integrated neutron scattering intensity can be fitted to experimental results in order to derive information about the exchange constants J and α.

Results like those given for mixed $S = 1/2$ chains (figures 3, 4) have been compared to very recent neutron scattering data on $Sr_{14}Cu_{24}O_{41}$ [13], where α is reported to be of the order of -0.1. We get perfect qualitative agreement of our expressions (8) and (18) with both the observed dispersion and the spectral weight. As the data have been taken at a rather low temperature ($T/J \approx 0.2$ in our notation), our theory underestimates α by about a factor of 2 compared to the theory used in the paper [17], which is valid at $T = 0$ and small values of α. However, we can clearly confirm the assumptions made by the authors of [13] about the intra-dimer and inter-dimer distances. We predict quite striking changes in the van Hove response as the temperature is increased.

For the ferromagnetic chain we believe our excitation spectrum to be accurate over the whole temperature range, as no gap can be expected in this case [10]. Our theory correctly shows a long-range ordered state at $T = 0$. To the best of our knowledge, there have been no experiments performed yet on ferromagnetic alternating chains.

Finally, we would like to remark that low-temperature properties of one-dimensional systems are generally difficult to investigate experimentally, as there will always be signatures of higher-dimensional interactions below a finite temperature. Given the increasing number of compounds found by ingenious manufacturing and the progress in experimental skills, one can be confident that many more experimental results on low-dimensional magnetic materials will emerge in the future.

Acknowledgments

One of us (SWL) worked on this study while a guest of Dr K N Trohidou at the National Centre for Scientific Research, 'Demokritos', with financial support from the EU through the contract ERBFMB1CT961209.

References

[1] Regnault L P, Aïn M, Hennion B, Dhalenne G and Revcolevschi A 1996 *Phys. Rev.* B **53** 5579
[2] Weiden M, Hauptmann R, Geibel C, Steglich F, Fischer M, Lemmens P and Güntherodt G 1997 *Z. Phys.* B **103** 1
[3] Lake B, Tennant D A, Cowley R A, Axe J D and Chen C K 1996 *J. Phys.: Condens. Matter* **8** 8613
[4] Garrett A W, Nagler S E, Tennant D A, Sales B C and Barnes T 1997 *Phys. Rev. Lett.* **79** 745
[5] Cowley R A, Lake B and Tennant D A 1996 *J. Phys.: Condens. Matter* **8** L179
[6] Lake B, Cowley R A and Tennant D A 1997 *J. Phys.: Condens. Matter* **9** 10 951
[7] Aïn M, Lorenzo J E, Regnault L P, Dhalenne G, Revcolevschi A, Hennion B and Jolicœur T 1997 *Phys. Rev. Lett.* **78** 1560
[8] Affleck I 1998 *Dynamical Properties of Unconventional Magnetic Systems* ed A T Skjeltorp and D Sherrington (Dordrecht: Kluwer) at press
[9] Cowley R A 1998 *Dynamical Properties of Unconventional Magnetic Systems* ed A T Skjeltorp and D Sherrington (Dordrecht: Kluwer) at press
[10] Bonner J C and Blöte H W J 1982 *Phys. Rev.* B **25** 6959

[11] Carter S A, Batlogg B, Cava R J, Krajewski J J, Peck W F Jr and Rice T M 1996 *Phys. Rev. Lett.* **77** 1378
[12] Matsuda M, Katsumata K, Eisaki H, Motoyama N, Uchida S, Shapiro S M and Shirane G 1996 *Phys. Rev.* B **54** 12199
[13] Eccleston R S, Uehara M, Akimitsu J, Eisaki H, Motoyama N and Uchida S 1998 *Phys. Rev. Lett.* submitted
[14] Manaka H, Yamada I and Yamaguchi K 1997 *J. Phys. Soc. Japan* **66** 564
[15] Hagiwara M, Narumi Y, Kindo K, Kobayashi T, Yamakage H, Amaya K and Schumauch G 1997 *J. Phys. Soc. Japan* **66** 1792
[16] Hida K 1994 *J. Phys. Soc. Japan* **63** 2514
[17] Harris A B 1973 *Phys. Rev.* B **7** 3166
[18] Kondo J and Yamaji K 1972 *Prog. Theor. Phys.* **47** 807
[19] Lovesey S W 1986 *Condensed Matter Physics: Dynamic Correlations* 2nd edn (Menlo Park, CA: Benjamin/Cummings)
[20] Richards P M 1971 *Phys. Rev. Lett.* **27** 1800
[21] Scales S A and Gersch H A 1972 *Phys. Rev. Lett.* **28** 917
[22] Auerbach A 1994 *Interacting Electrons and Quantum Magnetism* (New York: Springer)